JACS
JOURNAL OF THE AMERICAN CHEMICAL SOCIETY
Article
pubs.acs.org/JACS

Success in Making Zn^+ from Atomic Zn^0 Encapsulated in an MFI-Type Zeolite with UV Light Irradiation

Akira Oda,[†] Hiroe Torigoe,[†] Atsushi Itadani,[†] Takahiro Ohkubo,[†] Takashi Yumura,[‡] Hisayoshi Kobayashi,[‡] and Yasushige Kuroda*[,†]

[†]Department of Chemistry, Graduate School of Natural Science and Technology, Okayama University, 3-1-1 Tsushima, Kita-ku, Okayama 700-8530, Japan

[‡]Department of Chemistry and Materials Technology, Kyoto Institute of Technology, Matsugasaki, Sakyo-ku, Kyoto 606-8585, Japan

Supporting Information

ABSTRACT: For the first time, the paramagnetic Zn^+ species was prepared successfully by the excitation with ultraviolet light in the region ascribed to the absorption band resulting from the 4s−4p transition of an atomic Zn^0 species encapsulated in an MFI-type zeolite. The formed species gives a specific electron spin resonance band at g = 1.998 and also peculiar absorption bands around 38,000 and 32,500 cm^{-1} which originate from 4s−4p transitions due to the Zn^+ species with paramagnetic nature that is formed in MFI. The transformation process ($Zn^0 \rightarrow Zn^+$) was explained by considering the mechanism via the excited triplet state (^3P) caused by the intersystem crossing from the excited singlet state (^1P) produced through the excitation of the 4s−4p transition of an atomic Zn^0 species grafted in MFI by UV light. The transformation process was well reproduced with the aid of a density functional theory calculation. The thus-formed Zn^+ species which has the doublet spin state exhibits characteristic reaction nature at room temperature for an O_2 molecule having a triplet spin state in the ground state, forming an η^1 type of $Zn^{2+}-O_2^-$ species. These features clearly indicate the peculiar reactivity of Zn^+ in MFI, whereas $Zn^0-(H^+)_2$MFI hardly reacts with O_2 at room temperature. The bonding nature of $[Zn^{2+}-O_2^-]$ species was also evidenced by ESR measurements and was also discussed on the basis of the results obtained through DFT calculations.

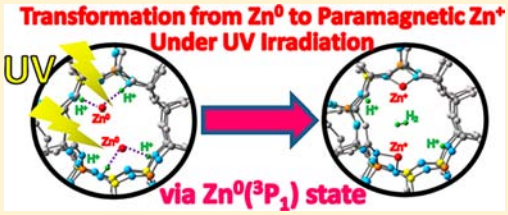

INTRODUCTION

In the group 12 elements, the dominant formal oxidation states are zerovalent and divalent states, and the important monovalent form is widely known only for mercury. In the case of zinc, it has been reported that a yellow diamagnetic glass composed of Zn_2^{2+} is obtained on cooling when Zn is added to molten $ZnCl_2$ at 773−973 K, although it seems that the evidence described in the paper is subtle in supporting the derived conclusions.[1] In addition, it should be noted that the formation of Zn_2^{2+} species in zeolite has been suggested.[2] Recently, another interesting compound, decamethyldizincocene, with a Zn−Zn bond, was prepared that has a curious +1 oxidation state for the respective zinc ions, as well as a diamagnetic nature.[3−6] This result is of particular interest in view of the fact that the monovalent state of zinc species is extremely unusual. However, it is not clear that two types of species really have a +1 nature or not in the cases including the dizinc species just described, because these exhibit a diamagnetic nature. Therefore, the preparation of a real monovalent zinc ion with a paramagnetic nature which is stable even at room temperature and information on its formation mechanism and reactivity are extremely desirable and essential from an inorganic chemistry viewpoint. The establishment of a preparation method in which the procedure is understood in detail and the elucidation of the characteristic features endowed on the thus-formed Zn^+ species are important issues in the field of inorganic chemistry and are indispensable for clarifying the reaction properties of Zn^+ for forthcoming molecules. To date, studies on the monovalent zinc ion have been carried out under extremely limiting conditions, such as γ-ray irradiation, and the formed species was characterized by the electron spin resonance (ESR) method.[7−9] The first report related to the preparation of Zn^+ species under mild conditions was published in 2003; however, its ESR spectrum scarcely supports the existence of the monovalent zinc species.[10] In 2011, that group also reported new results and succeeded in the preparation of Zn^+ species from Zn^{2+} exchanged in zeolite through electron transfer from the zeolite lattice to Zn^{2+}.[11] From their report, it is difficult for the present authors to consider that the zeolite lattice acts as such an efficient electron donor reagent toward the Zn^{2+} species. Furthermore, the formation of Zn^+ species has been very recently reported in ZnMFI prepared by the solid exchange method. In their case, little attention was given to the mechanism in the Zn^+ formation process.[12] The preceding paper by the same group was also published in 2012; they assumed the Zn^+ ion or $Zn^+-O^--Zn^{2+}$ species. However, the formation mechanism was not presented in their work, although it is very important from the viewpoint that the Zn^+ ion is a very novel and unprecedented state in inorganic compounds.[13]

Received: July 26, 2013
Published: November 13, 2013

dx.doi.org/10.1021/ja4077342 | J. Am. Chem. Soc. 2013, 135, 18481−18489

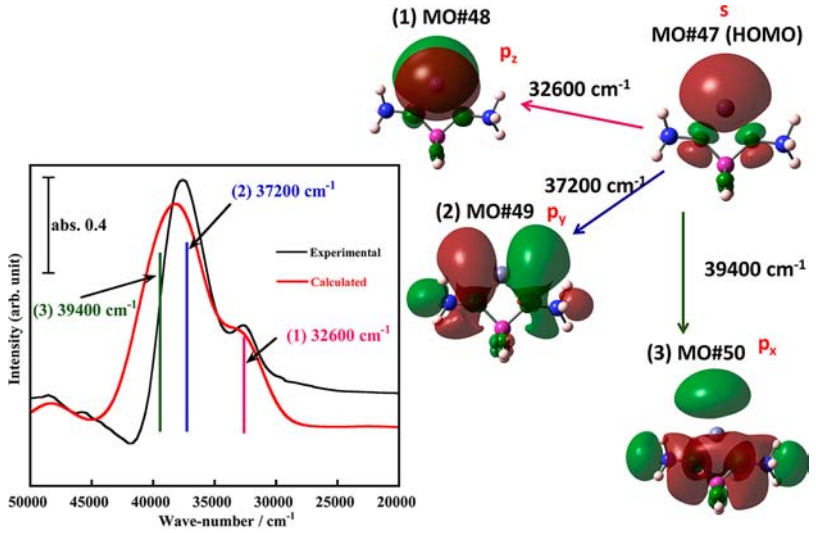

Figure 1. (a) Experimentally (black line) and theoretically (red line) obtained UV–vis DR spectra of $Zn^{I}MFI$, together with (b) the respective components (from 1 to 3) obtained by the TD-DFT calculations. For the experimental spectrum, the difference spectrum between the spectra measured before and after UV irradiation on the sample A is given. The original spectra are also given in Figure SI-1 (Supporting Information). The calculated spectrum is obtained by applying the TD-DFT method to the small model ($Zn^{I}AlSi_2O_4H_8$ unit). The fwhm of the reproduced spectrum was set to 2000 cm^{-1} in TD-DFT calculations.

We have also been investigating the specific behavior of metal ions exchanged into zeolite, which is quite different in nature from that found in bulk systems, and have found several peculiar adsorption features in the systems utilizing the zeolite lattice as the specific reaction field.[14−17] Very recently, we have discovered the exceptional and unprecedented nature of the divalent Zn ion exchanged in MFI-type zeolite, i.e. the formation of an atomic zinc species in MFI via a zinc hydride species resulting from the reaction with H_2, although it is generally accepted that metal species deposited on solid materials (catalysts) tend to be deactivated by the transformation of atomic species into metallic species in larger size (agglomeration) at higher temperatures.[18] In the case of ZnMFI, the zinc species in MFI is surprisingly amenable to agglomeration and keeps its atomic state even after treatment at higher temperatures. Therefore, by utilizing the atomic zinc species formed in MFI as the reaction field, the creation of a new type of electronic state on the solid surface is a significant issue and is indispensable for designing a new type of unprecedented reaction field. In this work, we aimed at preparing the paramagnetic monovalent zinc species by exciting the atomic zerovalent species formed in MFI, which exhibits strong absorption in the ultraviolet (UV) region by way of excitation of a 4s electron to the 4p state through irradiation with light in the UV region, and examining its reactivity.

■ RESULTS AND DISCUSSION

The ZnMFI-95 sample was first evacuated at 873 K, followed by treatment with H_2 at 573 K for 2 h at a pressure of 13.3 kPa, and finally evacuated at 300 K (sample A). This sample gives strong absorption bands in the region between 50000 and 33000 cm^{-1} in the diffuse reflectance (DR) spectrum in the UV–vis region, which is well explained by considering the electronic 4s−4p transition resulting from the formed atomic zinc metal species.[18] To determine the role of the triggering electron that evokes a marked effect on the reactivity of the atomic Zn species, we examined the effective excitation region for causing such spectral changes by altering the wavenumber of the irradiating light. Excitation by light including all absorptions resulting from the atomic zinc species brought about a clear change: the appearance of a band around 38000 cm^{-1} and a clear band at 32500 cm^{-1}, together with a decrease in intensity around 42000 cm^{-1} (Figure 1: black line). In contrast, irradiation with light cut off on the energy side higher than 25000 or 28570 cm^{-1} did not bring about any changes in the spectra (see the Supporting Information, Figure SI-1).

The UV activation process was followed by ESR measurements at 300 K (Figure 2a). Sample A, which includes an atomic Zn species, scarcely gave any ESR band (spectrum 1). After that, the sample was irradiated with light in different wavenumber regions between 50000 and 20000 cm^{-1}. This treatment brought about the appearance of a new ESR band with g = 1.998 having a symmetric nature depending on the wavenumber of the irradiated light (Figure 2a), which can be assigned to the Zn^+ species with a paramagnetic nature:[7−9] i.e., the formation of the Zn^+ species derived from Zn^0 under irradiation of light in a suitable region. Similar to the cases observed in the DR spectra, the band area of this ESR band increased stepwise under irradiation with light having higher energies (spectra from 2 to 8, Figure 2a). These data clearly indicate that irradiation in the region between 33000 and 50000 cm^{-1} is essential for producing this specific phenomenon. Once this species is formed through the irradiation of light, this ESR band is stable and does not lose its intensity after storage for a long time, which demonstrates the formation of stable Zn^+ species in MFI. For reference, only a slight amount of this ESR band was observed in the case of the heat-treatment procedure of Zn^0–$(H^+)_2$MFI at temperatures above 573 K: less than 1/100 in comparison with that for the light-irradiated sample. The effect of the efficient wavenumber of irradiated light on the appearance behavior of the ESR band ascribable to the Zn^+ species was also examined in a manner similar to that for the

dx.doi.org/10.1021/ja4077342 | J. Am. Chem. Soc. 2013, 135, 18481−18489

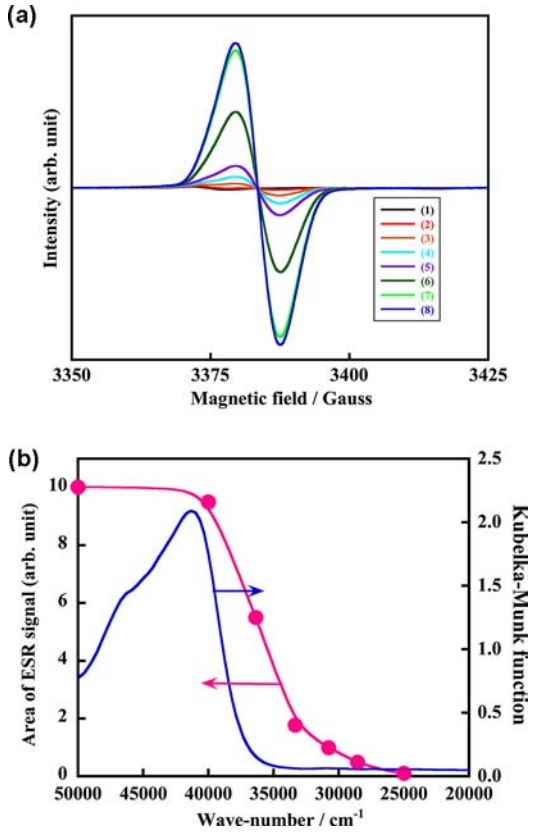

Figure 2. (a) ESR spectra of the sample treated under various conditions. The observed ESR band is attributable to the Zn^+ species. (1) The ZnMFI sample was first evacuated at 873 K, followed by treatment with H_2 at 573 K for 2 h under a pressure of 13.3 kPa, and finally evacuation at 300 K. The thus-prepared sample was irradiated with light having different wavenumbers lower than (2) 25000, (3) 28600, (4) 30800, (5) 33300, (6) 36300, (7) 40000, and (8) 50000 cm^{-1}, respectively. (b) Band areas of ESR signal corresponding to the respective spectra shown in Figure 2a, together with the absorption spectrum of the sample A, $Zn^0(H^+)_2$MFI-95.

measurements of DR spectra by changing the wavenumber of light, utilizing a narrow wavenumber interval for the excitation. The resulting relation between the band area observed in ESR and the light used in the excitation is plotted in Figure 2b. As a result, it is clearly evidenced that the excitation of the absorption region ascribable to the atomic zinc species is indispensable for causing the formation of Zn^+ species. It follows from the measurements of DR (Figure SI-1, Supporting Information) and ESR spectra (Figure 2a) that the excitation of the 4s electron of the Zn^0 species is essential for the formation of Zn^+ species from an atomic Zn^0 species formed in MFI. Accompanied by the formation of Zn^+, a decrease in the amount of the Brønsted acid site was also observed in the infrared (IR) spectrum (Figure SI-2, Supporting Information). On the basis of these data, we can propose the following reaction as the charge compensation mechanism resulting from the Zn^+ formation:

$$Z_A{-}O{-}H^+\cdots Zn^0\cdots H^+{-}O{-}Z_B \rightarrow Z_A{-}O{-}H^+ + Zn^+{-}O{-}Z_B + {}^1/_2H_2$$

where Z_A and Z_B represent the zeolite lattice including Al atoms.[19]

As described above, the behavior observed in the present DR and ESR spectra measurements can be interpreted in terms of the formation of Zn^+ in MFI through UV irradiation of $Zn^0{-}(H^+)_2$MFI. To clarify further the occurrence of this reaction (formation of Zn^+ species), we tried to reproduce the observed DR spectrum with the aid of a time-dependent density functional theory (TD-DFT) calculation. In our calculation, we constructed a small simpler model including a single Al atom on which a Zn^+ ion was positioned for compensation of the charge derived from the Al atom substituted for a Si atom; this cluster model is composed of the smallest $Zn^IAlSi_2O_4H_8$ unit (Figure 1), which is the simplest model terminated with $-O-SiH_3$ or $-O-Al(OH)_2$ in the peripheral parts. This model has been usually used for achieving the fundamental features of the metal-ion-exchanged MFI-type zeolite.[16−18,20−22] A TD-DFT calculation utilizing this smaller model was carried out to reproduce the observed DR spectrum. As a result, the calculated spectrum obtained by assuming a single Zn^+ species in this model is made up of the three dominant components (1) 32600, (2) 37200, and (3) 39400 cm^{-1}: (1) the transition from 4s to the $4p_z$ component of Zn^+, (2) that from 4s to $4p_y$ of Zn^+, although the latter component includes some contribution from the lattice atoms of oxygen, and (3) the transition from 4s to $4p_x$, which also contains some mixing with lattice oxygen atoms. These evaluated components of the dominant bands are shown in Figure 1b by the contour maps of the respective components of each transition. The calculated spectrum gives transitions between 30000 and 40000 cm^{-1} (Figure 1a, red curve), together with their components. As a result, the results from the DFT calculation assuming the formation of Zn^+ species give a good account of the UV−vis DR spectrum obtained experimentally.

To gain a better understanding of the transformation mechanism, an attempt to reproduce the process of changing from atomic Zn^0 in MFI to monovalent Zn ion was made by applying a DFT calculation to the present system. In the calculation, a larger model, a $Si_{92}O_{151}H_{66}$ cluster, was adopted as the MFI (silicalite) structure that could reasonably represent a 10-membered ring (10-MR) including the M7 site,[18] in which two Si atoms were replaced by two Al atoms to embody the ion-exchangeable site.[16−18,20−22]

In the present experiment, light in the absorption region between 50000 and 33000 cm^{-1} was efficiently utilized as an activation method that induces effectively the change in state from the zerovalent zinc to the monovalent state. We were able to assume two types of states as the dominant states, ^1P and ^3P, for the excited Zn species with zerovalent charge. First, we examined the Zn^0 (^1P) state as one of the possibilities: electron transition from the 4s level to the 4p level without change in the spin quantum number based on the selection rule, i.e., excitation from the ground state Zn^0 (^1S) to the excited state. However, in the calculation, there was absolutely no indication of a reaction by way of this state. Therefore, in the next step, we considered another possibility: the excited electron changes its spin state to the triplet state (^3P) by taking into account the existence of some relaxation process from the formed ^1P state through intersystem crossing. It may be possible to assume such a state by considering the large spin−orbit interaction[23] in Zn^0 that is supposed to be operating in the Zn−Xe, Zn−N_2, and Zn−CH_4 systems.[24−31] In such a circumstance, a spontaneous change to the monovalent species was observed in the present system (Figure 3, from step 1 to 24; Supporting Information, Figures SI-3 and SI-4) and finally results in the

dx.doi.org/10.1021/ja4077342 | J. Am. Chem. Soc. 2013, 135, 18481−18489

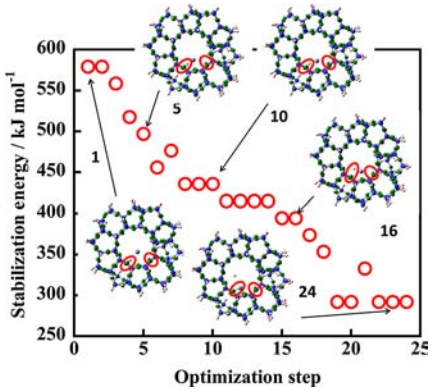

Figure 3. Energy relationship in the changing process from Zn^0 to Zn^+ by way of the ^3P state of an atomic zinc formed in MFI. The process was examined by applying DFT calculation methods to the MFI system utilizing the larger model $Zn^0Al_2Si_{90}O_{151}H_{68}$. The data are referred to the $Zn^0Al_2Si_{90}O_{151}H_{68}$ species as the zero value.

formation of both Zn^+ and $H^\bullet$ (radical); irradiation with UV light is essential for this reaction to take place. In the final structure $[Zn^I{-}(H^+)MFI + H^\bullet]$, formation of the Zn^+ ion was demonstrated and it was positioned substantially on the M7 site through interaction with the two oxygen atoms near the substituted Al atoms and the formed $H^\bullet$ species was floating in the MFI pore (Figure 3 and Figure SI-3). The distances between Zn^+ and the respective oxygen atoms in the final stage were evaluated as 1.96 and 2.39 Å (Figure SI-4), as well as the distance of O1−H1 being 5.36 Å, different from the O1−H1 distance of 0.98 Å in the initial stage. In addition, the energetic changes in the transformation process are also understandable from Figure 3. In this figure, the energy zero is taken as the energy for the larger cluster including $Zn^0(^1S)$, together with two H^+ ions existing near Al atoms for charge compensation (see also Figure SI-4).[18] The energy of the system spontaneously changes from the initial state including the ^3P state of Zn^0 just after excitation in the $Zn^0{-}(H^+)_2MFI$ to the stable state, $Zn^I{-}(H^+)MFI + H^\bullet$.

Prior to the lattice oxygen−Zn^+ bond formation, several processes will be depicted. Just after intersystem crossing from the ^1P state, the state becomes ^3P of Zn^0 (state 1) and this species exists in the MFI pore by interacting weakly with H1 and H2 with the bond lengths 2.71 Å for Zn−H1 and 3.12 Å for Zn−H2 (Figure SI-4, Supporting Information). The bond distances of Zn^0 with O1 and OL (lattice oxygen) were evaluated as 3.67 and 3.77 Å, respectively. In this condition, the structure of state 1 is the same as that evaluated in the previous work for Zn^0, which has a ^1S state, because it is only a presumed temporary state in the calculation process; the electronic transition between two states, i.e., an $^1S \rightarrow {}^1P$ transition, takes place so rapidly that there is no change in the configurational coordinate, in accordance with the Franck−Condon principle.[18] This state (step 1) is followed by relaxation in the electronic and structural states to the stable and genuine ^3P state around step 5. By way of several steps from step 1, Zn^0 gradually changes its initial position and approaches the lattice oxygens, OL (2.86 Å) and O1 (2.79 Å), concurrently maintaining the distances with H1 (1.75 Å) and H2 (2.86 Å). In step 10, Zn^0 is brought closer to O1 (2.62 Å) and OL (2.18 Å), resulting in the distance from H2 shortening (2.33 Å), although the H1 position almost maintains the distance with Zn^0 at 1.76 Å, which is almost the same as that found in step 5. In this stage, the Zn^0 species experiences a five-body interaction among atoms, ions, and metal: i.e., O (lattice oxygen atoms, O1 and OL), H^+ (H1), H^+ (H2), and Zn^0. In the next stage (step 11), a change in the state of Zn^0 eventually takes place and it influences the magnitude of the contribution to the bonding nature between O and H^+; Zn^0 is rather remote from the oxygen atoms, O1 (2.75 Å) and OL (2.32 Å), and the interaction with both H^+'s, H1 (1.65 Å) and H2 (2.28 Å), again increases in strength. This is presumably caused by the change in the interaction from the dominant p character to the s character in Zn (as shown below); redistribution of the electron and formation of the Zn^+ species take place continuously. Subsequently (step 16), the formed Zn^+ species interacts strongly with atoms with an electronegative nature, O1 and OL, beginning the weakening in the bond strength between O1 and H1. In the final stage (step 24), it is found that the bond between the Zn^+ ion and lattice oxygen atoms is clearly formed, simultaneously accompanied by the reduction of H^+ to $H^\bullet$ (shown in the latter part). As a result, a further increase in the strength of the interaction of Zn^+ with oxygen atom O1 (1.96 Å) and a concomitant decrease in the interaction with OL (2.39 Å) were observed, and simultaneously the formed $H^\bullet$ leaves the surface of the zeolite lattice for the center of the pore (O1−H1 = 5.36 Å), as is shown in Figure SI-4. It is important to note that the energy of step 10 is evaluated to be almost 430 kJ/mol

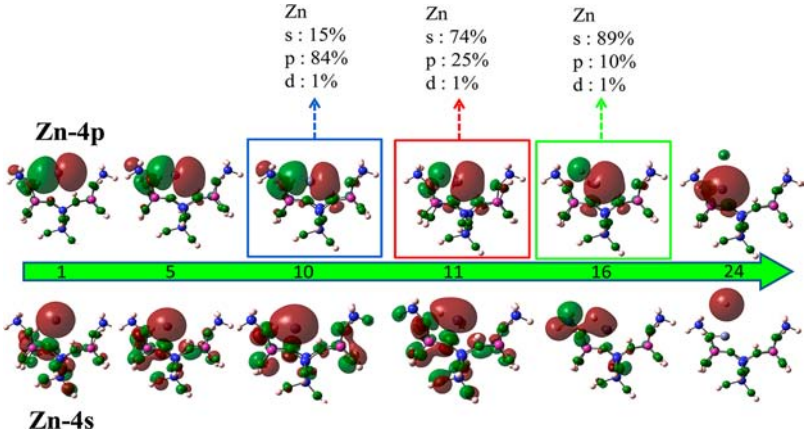

Figure 4. Variation of molecular orbitals of the dominant Zn 4p and Zn 4s orbitals in the changing process from Zn^0 to Zn^+ shown in Figure 3. In this calculation, the medium model $ZnAl_2Si_7O_{19}H_{18}$ is used.

dx.doi.org/10.1021/ja4077342 | J. Am. Chem. Soc. 2013, 135, 18481−18489

higher than that for the original state as the reference state, energy zero: (Zn^0 + $2H^+$) in MFI. This value corresponds well with the required energy for excitation to the ^3P state.[31]

The bonding nature in the processes from step 1 to step 24 was also examined on the basis of molecular orbital (MO) calculation methods. The dominant MO contribution (contour maps) operating in the new bond-formation processes, from states 1 to 24, steps 1, 5, 10, 11, 16, and 24, are given in Figure 4. In these processes, it is found that both Zn 4p and Zn 4s orbitals play pivotal roles in the present phenomenon. For the case including the ground state of an atomic Zn^0, Zn 4s, which is the highest occupied molecular orbital (HOMO) level, is doubly occupied: zero spin (singlet, ^1S). As described above, we assumed that the excited triplet state (^3P) is created by UV light irradiation by way of the excited singlet state (^1P); the electrons dominantly occupied both Zn 4p and Zn 4s with parallel spin states (^3P: α-spin). This assumed state is the transient state. Therefore, we focus on these two orbital states. More detailed MOs composed of 4s and 4p are also given in Figure SI-5 (Supporting Information). In the first step, the Zn 4s orbital is mainly made up of the dominant component of the 4s orbital of Zn^0 and is occupied with α-spin. In contrast, Zn 4p with α-spin dominantly combined with the orbital composed of a larger contribution from the H1 orbital, which includes some contribution from the lattice oxygen atom, as shown in Figure 4 and Figure SI-5a (step 1). The changing process was also represented by considering the spin density of the system (Figure 5). In the initial step, the excited zinc atom, especially $4s^1$ and $4p^1$, takes a high spin density (^3P), indicating that the unpaired electrons are localized on the zinc atom in the initial state (just after excitation), which can be said that the zinc atom takes the pseudo triplet state in conformity with our view. This transient state is gradually transformed, and consequently both MO orbitals in step 5 are almost the same as those found in step 1 (initial state), although Zn^0 slightly changes its position and interacts strongly with H^+, especially H1, and simultaneously with O1 and OL (Figure 4 and Figure SI-4). Spin change in the steps from 1 to 4 seems to be attributable to a relaxation process caused by the sudden change from the state ^1P to the state ^3P used in calculations, as mentioned in the previous part. After that, the interaction of Zn with H2 seems to be slightly strengthened in step 10 by interaction through Zn 4p (see also Figure SI-5b), accompanied by a shortening in the bond length with OL. Information on the bond length is also given in Figure SI-4. These processes appear to be the stabilizing processes of the triplet state (Figure 3). After that, Zn^0 comes closer to both H1 and H2 in step 11 (Figures SI-4 and SI-5c), and simultaneously a decrease in the contribution of p character in Zn takes place (Figures 4 and 5). In this stage, the phase of the orbital between H1 and Zn shows its antibonding nature (Figure 4 and Figure SI-5c), and concurrently an increase in the s character of the formed Zn^+ ion was clearly observed, together with the interaction with H2: a change from the triplet spin state to two kinds of doublet states, H and Zn^+ (Figure 5), and concurrent formation of Zn^+. Striking changes in the amount of spin densities takes place for α spin on the Zn 4p orbital between steps 10 and 13, which were accompanied with a simultaneous increase in the density in the Zn 4s orbital (Figure 5a(1)). This change corresponds to the decrease in p character in the original Zn 4p and concurrently the decrease in the electron distribution in the original Zn 4s orbital takes place, followed by an increase in the density in H1 1s (Figure 5a(2)). As a result, the phenomenon

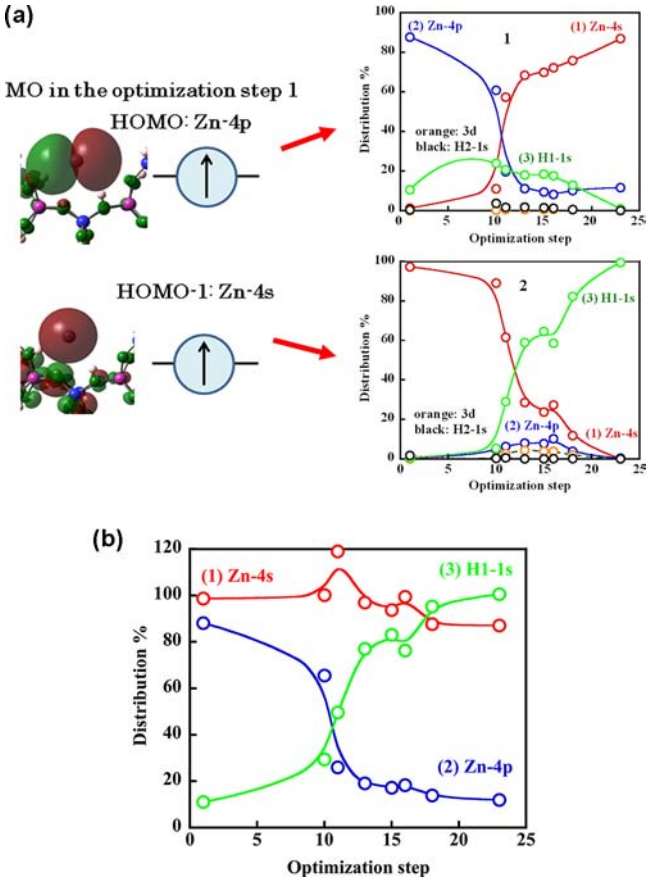

Figure 5. Variation of total amounts of the spin distribution of the dominant components in the changing process from Zn^0 to Zn^+ encapsulated in MFI-type zeolite in the optimization steps. These changing processes of the structure, as well as molecular orbitals, are depicted in Figures 3 and 4. (a) Spin distribution in respective orbitals. 1, the HOMO orbital constituted of the dominant component, Zn 4p, in the initial state; 2, the orbital (HOMO-1) composed of the dominant component, Zn 4s, in the initial state. (b) Comparison of total amounts of the spin densities in the respective orbitals of (1) Zn 4s, (2) Zn 4p, and (3) H1 1s. The respective spin distribution probabilities are obtained by summing up the data shown in Figure 5a. In both parts, the ordinate values are depicted in the ratio of the spin distribution in the respective orbitals.

can be apparently interpreted in terms of electron transfer from Zn 4p to H1 1s (Figure 5b). The substantial electron transfer from the ^3P state of Zn^0 to H1 would take place in the steps from 10 to 13. After this stage, the phase of the orbital between H1 and Zn^+ having 4s nature became more antibonding (step 16: Figure 4 and Figure SI-5d), resulting in an exchange in the position of H1 with Zn^+. Simultaneously, the thus-formed Zn^+ weakens the interaction with H2 and leaves its position and approaches O1. Another important addition to be made to what we have said about the observed behavior is that there is little change in the spin component composed of H2 1s and Zn 3d orbitals in all changing steps, as shown in Figure 5a(1,2). It is clearly understandable from Figure 5b that the spin density which exists in the 4p orbital in the initial state was transferring to the H1 1s orbital in the final stage without changing the spin density in the Zn 4s orbital. Finally, the original Zn 4p orbital takes on 4s nature and concurrently the 4s electron transferred to H1 1s, which leaves from the position connected with the

dx.doi.org/10.1021/ja4077342 | J. Am. Chem. Soc. 2013, 135, 18481−18489

zeolite lattice. As a result, oxidation of Zn^0 to Zn^+ takes place, together with the formation of an atomic H species (Figure 5).

To gain information on the reactivity of the formed Zn^+ species, we examined the activation of O_2 at room temperature. Activation of O_2 is important in nature and in industrial chemistry, as shown by the key role of oxidation in biochemistry and in the production of value-added compounds.[32,33] In addition, reactive oxygen species adsorbed at surfaces are important intermediates in both total and selective catalytic oxidation.[34−37] However, only in a few cases is the O_2^- species formed on a substantially unperturbed surface. In the present experiment performed after the formation of Zn^+ in MFI, the adsorption of O_2 was carried out at 300 K, resulting in the disappearance of the ESR band assigned to Zn^+ (g = 1.998), accompanied by the appearance of another type of spectral pattern composed of the dominant anisotropic g parameters g_{xx} = 2.0033, g_{yy} = 2.0108, and g_{zz} = 2.0339 (Figure 5, spectrum 1). The resulting simulated spectrum is also given in Figure 6

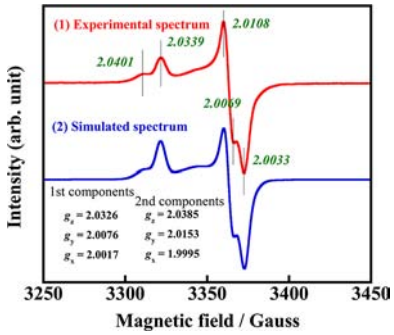

Figure 6. ESR spectra of the Zn^IMFI sample measured at room temperature: (1) spectrum of the sample treated with O_2 at 300 K, followed by re-evacuation at 300 K; (2) simulated spectrum, together with respective g values.

(spectrum 2). This process also caused changes in the DR spectra; the bands that are assigned to Zn^+ species completely lost their intensities (Figure SI-6, Supporting Information). Taking these data into consideration, the ESR signal observed after O_2 adsorption can be assigned to the O_2^- (superoxide) ion formed by the following interaction: the electron in the 4s orbital of Zn^+ is partially transferred to a partially occupied π^* orbital.[38−41] The present model is not in conflict with the result obtained from ESR data shown above.[36] As a result, it is the Zn^+ ion that exhibits a prominent reaction nature for the O_2 molecule with the triplet state.[42]

To obtain information on the bonding interaction between Zn^+ and O_2, the transferring mechanism of the electron from Zn^+ ion bound to two framework oxygen atoms near the substituted Al atom toward the O_2 molecule was evaluated on the basis of the MO interaction. In the calculation, we adopted the smallest MFI model (i.e., a $Zn^IAlSi_2O_4H_8$ cluster) and examined the formation process of the $[Zn^IAlSi_2O_4H_8{-}O_2]$ species. In the calculation, an O_2 molecule was initially positioned at a distant point (ca. 3.5 Å) from the exchanged Zn^+ ion in the small model mimicking MFI. After optimization, one of the oxygen atoms was interacting with a Zn^+ species: the formation of an η^1 type of $Zn^{2+}{-}O_2^-$ species. Taking account of the results reported by Bedilo et al.,[36] the present data concerning the g values obtained well support the formation of an η^1-type interaction. As for the interaction between Zn^+ and O_2, the formation of hybridization among 3d, 4s, and π^* orbitals is associated with the closeness of these energy levels. The relative energies of these levels of both a free O_2 molecule and Zn^+ in the small cluster model as the zeolite are shown in Figure 7. Taking account of the relation of energy levels among

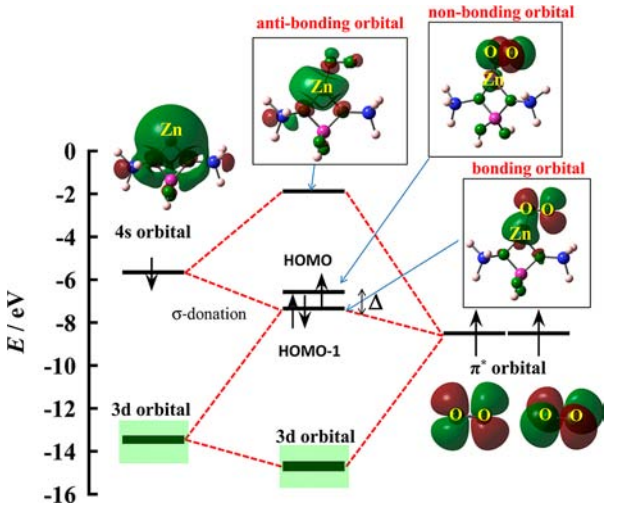

Figure 7. Molecular orbitals and their energy relationship in the bond-formation process of Zn^+ ion exchanged in MFI with the O_2 molecule. The process was examined with the aid of DFT calculation methods. In this calculation the smaller cluster model $Zn^IAlSi_2O_4H_8$ was used as the MFI model.

3d(Zn), 4s(Zn), and $\pi^*(O_2)$ orbitals, the levels resulting from the interaction between these orbitals are stabilized and the electron in the 4s orbital having a higher energy, in comparison with the level of $2\pi^*$ orbitals of O_2, is spontaneously transferred toward one of the π^* orbitals (σ donation), causing the spontaneous formation of the superoxide ion. As a result, an easy reaction with O_2 took place at room temperature in the present system.

As given in Tables 1 and 2, natural population analysis showed that ca. 0.7−0.8 of an electron from the Zn^+ ion transfers to the O_2 molecule through the interaction between 4s and π^* orbitals, resulting in the formation of $Zn^{2+}{-}O_2^-$ (Figure

Table 1. Structural Parameters for the Optimized Structure of Zn^+ by Utilizing the Small Cluster Model: (1) before and (2) after O_2 Adsorption

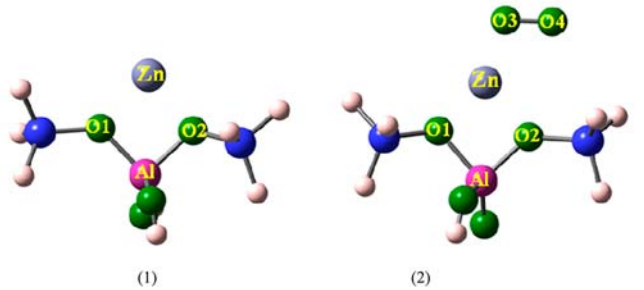

$E_{ads.}$ = −150 kJ mol^{-1}; $\nu_{(O-O)}$ = 1115 cm^{-1}.

	bond distance/Å				
	Zn−O1	Zn−O2	Zn−O3	Zn−O4	O3−O4
(1) before O_2 adsorption	2.04	2.01			1.21
(2) after O_2 adsorption	1.97	1.90	1.86	2.57	1.33

dx.doi.org/10.1021/ja4077342 | J. Am. Chem. Soc. 2013, 135, 18481−18489

Table 2. Calculated Electron Density for the Optimized Structure of Zn^+ by Utilizing the Small Cluster Model: (1) before and (2) after O_2 Adsorption

	Electron density		
	Zn	O3	O4
(1) before O_2 adsorption	[core] 4s (1.12)	—	—
	3d (9.98) 4p (0.01)		
(2) after O_2 adsorption	[core] 4s (0.47)	[core] 2s (1.82)	[core] 2s (1.85)
	3d (9.94) 4p (0.01)	2p (4.69)	2p (4.35)
O_2 molecule	—	[core] 2s (1.80)	[core] 2s (1.80)
		2p (4.17)	2p (4.17)

7). Another π^* orbital in the O_2 molecule interacts weakly with the Zn ion. Such a type of interaction stabilized the $[O_2{-}Zn]^+$ complex by 150 kJ mol^{-1} in comparison with the data for the reference state including Zn^+ and O_2 independently. As for the bond distance between the oxygen atoms, the evaluated bond length increased from 1.21 Å in the initial state to almost 1.33 Å in the final state. Taking account of the data reported so far, the evaluated bond length of ca. 1.33 Å in the final state enables us to assign the ligated dioxygen species to the superoxide category.[43] For confirmation, we evaluated the wavenumber for the superoxide ion formed in the final state on the basis of the calculation procedure, resulting in a value of 1115 cm^{-1}. The correlation between bond length of O−O and the wavenumber of its stretching vibration, both measured and calculated, gives a near-linear relationship.[32] The evaluated values (1.33 Å and 1115 cm^{-1}) follow a point on the straight line, falling into the category of superoxide ion in accordance with the experimental data.

On the basis of the model described above, a hole resides in the π^* (HOMO) because of the slight splitting, Δ, in energy through the interaction with the Zn ion. According to studies reported previously,[44−46] the g values of the O_2^- molecular ion are related to the crystal splitting (Δ) between HOMO and HOMO-1 levels, the spin−orbit coupling constant (λ) for the superoxide ion, and a correction for the angular momentum (l) caused by the crystal field. Assuming l = 1.00 and using the λ value of 153 cm^{-1}, Δ can be evaluated to be ca. 10000 cm^{-1}. The value is also compared with the datum evaluated by applying the DFT calculation based on the proposed model, providing a value of 6300 cm^{-1} (Figure 7).

As a result, all experimental data are explained reasonably by the model proposed in the present work.

CONCLUSIONS

We have succeeded in the preparation of a stable Zn^+ species with a paramagnetic nature through the activation of an atomic Zn^0 species encapsulated in an MFI-type zeolite with UV light in the region ascribed to the 4s−4p transition of an atomic Zn^0 species. The transformation process from Zn^0 to Zn^+ in MFI was accompanied by a simultaneous decrease in intensity of the IR band (3611 cm^{-1}) attributable to the Brønsted acid site, i.e., reduction in the amounts of H^+, arising from the additional charge generation accompanied by the formation of the Zn^+ species $Z_A{-}O{-}H^+{\cdots}Zn^0{\cdots}H^+{-}O{-}Z_B \rightarrow Z_A{-}O{-}H^+ + Zn^+{-}O{-}Z_B + {}^1/_2H_2$, where Z_A and Z_B represent the zeolite lattice including Al atoms. The transformation process ($Zn^0 \rightarrow Zn^+$) was well explained by considering the mechanism by way of the excited triplet state (^3P) caused by the intersystem crossing from the excited singlet state (^1P) of an atomic Zn^0 grafted in MFI with UV light irradiation. The thus-formed Zn^+ species, which has a doublet spin state, exhibits the characteristic reaction nature at room temperature for an O_2 molecule having a triplet spin state in the ground state, forming a superoxide ion, which is associated with the formation of an η^1 type of $Zn^{2+}{-}O_2^-$ species through the interaction of Zn^+ formed in MFI with O_2, whereas the $Zn^0{-}(H^+)_2$MFI hardly reacts with O_2 at room temperature. These features clearly indicate the peculiar reactivity of Zn^+ in MFI. Mononuclear metal−dioxygen adducts ($M{-}O_2$), such as end-on and side-on metal O_2 species, are generated in the O_2 activation and are critical components of the processes leading to practical substrates in oxidative transformations; they work as key intermediates in the oxidation of organic substrates. These findings reported in this work imply the potential for the specificity of Zn^+ encapsulated in MFI and its catalytic peculiarity in oxidation reactions for organic materials.

EXPERIMENTAL SECTION

Materials. Approximately 5 g of a sodium-type MFI zeolite (NaMFI) with a Si/Al ratio of 11.9, which was purchased from Tosoh Co., was dispersed in an aqueous solution of 0.3 M $Zn(NO_3)_2$ at room temperature. The composition of zinc-ion-exchanged zeolites (ZnMFI − X) can be expressed as follows: $Zn_{3.72X/100}Na_{7.44(100-X)/100}Al_{7.44}Si_{88.56}O_{192}{\cdot}nH_2O$, and the notation X denotes the ion-exchange level in percent (%) on the basis of the above composition. A sample having an ion-exchange level of 95% was used in the present experiment.[18]

Methods. We used various experimental methods, such as measurements of IR, DR, and ESR spectra, and also theoretical calculations utilizing the DFT method.

Measurement of IR Spectra. The sample (ca. 6 mg) was pressed under a pressure of 120 kg cm^{-2} into a disk of diameter of 10 mm and set in an in situ cell equipped with KRS-5 windows.[18] After the sample was evacuated at 873 K for 2 h, H_2 gas was introduced to the system. IR spectra were recorded in the transmission mode at room temperature using a Digilab FTS-4000MXK FTIR spectrophotometer equipped with a triglycine sulfate (TGS) detector.

DR Spectra. UV−vis−near-IR DR spectra were recorded at 300 K in the wavenumber range of 50000−4000 cm^{-1} using a spectrophotometer (Jasco V-570) equipped with an integral sphere attachment to obtain the DR spectra of the samples. The powdered sample was placed in a vacuum reflectance cell made of fused silica. Spectralon (Labsphere, North Sutton, NH, USA) was used as the reference material.

ESR Spectra. The ESR spectra were recorded in the X-band (ca. 9.5 GHz) at both 300 and 4 K with a JEOL JES-FA200 spectrometer equipped with a variable low-temperature apparatus (ES-CT470). All ESR measurements were carried out under in situ conditions for every sample. g values were determined by reference to the spectrum of Mn^{2+} doped into MgO as a standard.

Computational Methodology (Calculation Method). In the present study, we used one of the most successful hybrid Hartree−Fock/DFT methods, implemented in the Gaussian 03 and 09 program packages.[47] The B3LYP method[48−51] was used in this study. In general, the hybrid B3LYP method is well-known to provide excellent

dx.doi.org/10.1021/ja4077342 | J. Am. Chem. Soc. 2013, 135, 18481−18489

descriptions of various properties.[52] As a model of the MFI-type zeolite (for the 10-membered ring: 10-MR), we adopted an $Al_2Si_{90}O_{151}H_{68}$ cluster, where the terminal atoms are bound by H atoms. This model contains the basic part of the MFI framework explicitly comprised of MFI 10-MR.[53] A previous study confirmed that the B3LYP-optimized MFI model has 10-MR cavities and it well reproduces the data observed experimentally.[22] As for other small models, we first optimized the larger model. After optimization, we truncated the medium cluster in the positions of the M7 sites ($ZnAl_2Si_7O_{19}H_{18}$) from larger clusters, which are terminated by $-Si(OH)_3$, and used the M7 (6-MR) site with specified Al configurations to determine the most stable states in the respective sites. The 6-311G(d) basis set was used for H^+ and Zn atom or Zn ions, the 6-31G(d) basis set was used for the nearest Al and O atoms, and the 3-21G(d) basis set was used for other atoms. Despite the limitations of computational resources, we confirmed previously that B3LYP calculations with the same basis sets can well reproduce experimental IR vibrational frequencies of methane deformed by interactions with CuMFI.[16]

After the optimizations of an O_2 molecule adsorbed on Zn^+−MFI, we evaluated the stabilization energy of the O_2-adsorbed species. We also focused on how the O_2 molecule interacts with a cation within a small model surface of MFI, $Zn^IAlSi_2O_4H_8$. In order to evaluate the IR spectrum of adsorbed O_2, a vibrational analysis was performed for the optimized structure. The adsorption energies were obtained from the difference between the total energies of the systems, including a free O_2 molecule and including an adsorbed O_2 molecule. In general, theoretical harmonic frequencies overestimate experimental values because of incomplete descriptions of electron correlations and neglect of mechanical anharmonicity. To compensate for this problem, a uniform scaling factor of 0.962 was applied to the calculated frequencies obtained at the B3LYP level of theory, as recommended by Andersson and Uvdal.[54]

TD-DFT. The TD-DFT calculations were also carried out utilizing the Gaussian 09 software package. In this work, the TD-DFT approach was applied to analyze the photoabsorption spectra of both Zn^+-ion-exchanged species and the formed zinc metal species in MFI-type zeolite. To obtain photoabsorption spectra of the monovalent zinc ion formed inside the MFI model, we used the 6-311G(d) basis set for the H^+ ions and the LanL2DZ for the Zn^+ species, the 6-31G(d) basis set for the Al and O atoms that are bonded to the substituted Al atom, and the 3-21G(d) basis set for other atoms in the adopted models.

■ ASSOCIATED CONTENT

Ⓢ Supporting Information

Text describing changes in the DR UV−vis spectrum through UV light irradiation and figures giving UV−vis DR spectra of the ZnMFI-95 sample treated under various conditions, IR spectra measured before and after UV irradiation on sample A (ZnMFI-95), as well as their difference spectrum, the changing process from atomic Zn^0 to Zn^+ in MFI-type zeolite, structural information on the changing process, dominant MOs in the changing process, and UV−vis DR spectra of Zn^IMFI by way of irradiation with UV light onto $Zn^0(H^+)_2MFI$ and of subsequent O_2 treatment at room temperature. This material is available free of charge via the Internet at http://pubs.acs.org.

■ AUTHOR INFORMATION

Corresponding Author

kuroda@cc.okayama-u.ac.jp

Notes

The authors declare no competing financial interest.

■ ACKNOWLEDGMENTS

Financial support was provided by the Japan Society of Promotion Science (Grants-in-Aid for Scientific Research: No. 21655021). This research was also supported in part from a new project led by Prof. Y. Kubozono of Okayama University. H.T. and A.O. acknowledge financial support from the Japan Society for the Promotion of Science (Research Fellowship for Young Scientists, DC1).

■ REFERENCES

(1) Kerridge, D. H.; Tariq, S. A. *J. Chem. Soc. A* **1967**, 1122−1125.
(2) Rittner, F.; Seidel, A.; Boddenberg, B. *Microporous Mesoporous Mater.* **1998**, *24*, 127−131.
(3) Resa, I.; Carmona, E.; Gutierrez-Puebla, E.; Monge, A. *Science* **2004**, *305*, 1136−138.
(4) Schnepf, A.; Himmel, H.-J. *Angew. Chem., Int. Ed.* **2005**, *44*, 3006−3008.
(5) Carmona, E.; Galindo, A. *Angew. Chem., Int. Ed.* **2008**, *47*, 6526−6536.
(6) Li, T.; Schulz, S.; Roesky, P. W. *Chem. Soc. Rev.* **2012**, *41*, 3759−3771.
(7) Moorthy, P. N.; Weiss, J. J. *Nature* **1964**, *201*, 1317−1318.
(8) Isoya, J.-I.; Fujiwara, S. *Bull. Chem. Soc. Jpn.* **1972**, *45*, 2182−2188.
(9) Popescu, F. F.; Grecu, V. V. *Solid State Commun.* **1973**, *13*, 849−751.
(10) Tian, Y.; Li, G.-D.; Chen, J.-S. *J. Am. Chem. Soc.* **2003**, *125*, 6622−6623.
(11) Li, L.; Li, G.-D.; Yan, C.; Mu, X.-Y.; Pan, X.-L.; Zou, X.-X.; Wang, K.-X.; Chen, J.-S. *Angew. Chem., Int. Ed.* **2011**, *50*, 8299−8303.
(12) Qi, G.; Xu, J.; Su, J.; Chen, J.; Wang, X.; Deng, F. *J. Am. Chem. Soc.* **2013**, *135*, 6762−6765.
(13) Xu, J.; Zheng, A.; Wang, X.; Qi, G.; Su, J.; Du, J.; Gan, Z.; Wu, J.; Wang, W.; Deng, F. *Chem. Sci.* **2012**, *3*, 2932−2940.
(14) Itadani, A.; Tanaka, M.; Mori, T.; Nagao, M.; Kobayashi, H.; Kuroda, Y. *J. Phys. Chem. C* **2007**, *111*, 12011−12023.
(15) Kuroda, Y.; Okamoto, T.; Mori, T.; Yoshikawa, Y. *Chem. Lett.* **2004**, *33*, 1580−1581.
(16) Itadani, A.; Sugiyama, H.; Tanaka, M.; Ohkubo, T.; Yumura, T.; Kobayashi, H.; Kuroda, Y. *J. Phys. Chem. C* **2009**, *113*, 7213−7222.
(17) Torigoe, H.; Mori, T.; Fujie, K.; Ohkubo, T.; Itadani, A.; Gotoh, K.; Ishida, H.; Yamashita, H.; Yumura, T.; Kobayashi, H.; Kuroda, Y. *J. Phys. Chem. Lett.* **2010**, *1*, 2642−2650.
(18) Oda, A.; Torigoe, H.; Itadani, A.; Ohkubo, T.; Yumura, T.; Kobayashi, H.; Kuroda, Y. *Angew. Chem., Int. Ed.* **2012**, *51*, 7719−7723.
(19) The Zn ion with the prominent feature described in this work is restricted to the ion-exchanged species on the M7 site with S2 configuration as clarified in a previous work.[18] From the experiment of the adsorption measurements, the amounts of H_2 adsorbed dissociatively on ZnMFI, which is the same sample used in the previous work (95% ion exchanged ZnMFI: ZnMFI-95), are evaluated to be ca. 15% of the total amount of the exchanged Zn^{2+} in ZnMFI-95. Therefore, the amount of Zn^+ transferred from Zn^0 corresponds to this amount as the maximum value. The data evaluated with the aid of a few kinds of experiments, including the data shown in Figure SI-1 (Supporting Information), qualitatively give real amounts of formed Zn^+ species to be ca. 20−40% of the total amounts of an atomic zinc species. However, an accurate evaluation of the amount of the formed Zn^+ is difficult at the present stage.
(20) Yumura, T.; Yamashita, H.; Torigoe, H.; Kobayashi, H.; Kuroda, Y. *Phys. Chem. Chem. Phys.* **2010**, *12*, 2392−2400.
(21) Yumura, T.; Nanba, T.; Torigoe, H.; Kuroda, Y.; Kobayashi, H. *Inorg. Chem.* **2011**, *50*, 6533−6542.
(22) Yumura, T.; Takeuchi, M.; Kobayashi, H.; Kuroda, Y. *Inorg. Chem.* **2009**, *48*, 508−517.
(23) Francisco, E.; Pueyo, L. *Phys. Rev. A* **1987**, *36*, 1978−1982.
(24) Breckenridge, W. H. *Acc. Chem. Res.* **1989**, *22*, 21−27.
(25) Wallace, I.; Kaup, J. G.; Breckenridge, W. H. *J. Phys. Chem.* **1991**, *95*, 8060−8065.

(26) Castillo, S.; Rammirez-Solis, A.; Diaz, D.; Poulain, E.; Novaro, O. *Mol. Phys.* **1994**, *81*, 825−836.
(27) Greene, T. M.; Andrews, L.; Downs, A. J. *J. Am. Chem. Soc.* **1995**, *117*, 8180−8187.
(28) Breckenridge, W. H. *J. Phys. Chem.* **1996**, *100*, 14840−14855.
(29) McCaffrey, J. G.; Kerins, P. N. *J. Chem. Phys.* **1997**, *106*, 7885−7898.
(30) Bracken, V. A.; Gürtler, P.; McCaffrey, G. *J. Phys. Chem. A* **1997**, *101*, 9854−9862.
(31) Colmenares, F.; McCaffrey, J. G.; Novaro, O. *J. Chem. Phys.* **2001**, *114*, 9911−9918.
(32) Cramer, C. J.; Tolman, W. B.; Theopold, K. H.; Rheingold, A. L. *Proc. Natl. Acad. Sci. U.S.A.* **2003**, *100*, 3635−3640.
(33) Cho, J.; Sarangi, R.; Nam, W. *Acc. Chem. Res.* **2012**, *45*, 1321−1330.
(34) Lunsford, J. H.; Jayne, J. P. *J. Chem. Phys.* **1966**, *44*, 1487−1492.
(35) Iyengar, R. D.; Subba Rao, V. V. *J. Phys. Chem.* **1971**, *75*, 3089−3092.
(36) Bedilo, A. F.; Plotnikov, M. A.; Mezentseva, N. V.; Volodin, A. M.; Zhidomirov, G. M.; Rybkin, I. M.; Klabunde, K. J. *Phys. Chem. Chem. Phys.* **2005**, *7*, 3059−3069.
(37) Machida, M.; Murata, Y.; Kishikawa, K.; Zhang, D.; Ikeue, K. *Chem. Mater.* **2008**, *20*, 4489−4494.
(38) Kieber-Emmons, M. T.; Annaraj, J.; Seo, M. S.; Van Heuvelen, K. M.; Tosha, T.; Kitagawa, T.; Brunold, T. C.; Nam, W.; Riordan, C. G. *J. Am. Chem. Soc.* **2006**, *128*, 14230−14231.
(39) Cho, J.; Woo, J.; Nam, W. *J. Am. Chem. Soc.* **2010**, *132*, 5958−5959.
(40) Lee, Y.-M.; Hong, S.; Morimoto, Y.; Shin, W.; Fukuzumi, S.; Nam, W. *J. Am. Chem. Soc.* **2010**, *132*, 10668−10670.
(41) Peterson, R. L.; Himes, R. A.; Kotani, H.; Suenobu, T.; Tian, L.; Siegler, M. A.; Solomon, E. I.; Fukuzumi, S.; Karlin, K. *J. Am. Chem. Soc.* **2011**, *133*, 1702−1705.
(42) In order to specify the reaction of O_2 with Zn^+, we examined the reaction of O_2 with atomic zinc, Zn^0, with the aid of DFT calculation methods. In this calculation, an O_2 molecule is initially positioned at the distance of 2.5 Å from Zn^0, which is shorter than that for the case of Zn^+ described in the text, and successively the optimization was carried out. In this case, O_2 was leaving from the Zn^0 species, indicating that the reaction is scarcely taking place in the O_2−Zn^0 system. This fact is well consistent with the experimental results: ESR, UV−vis DR, and XAFS measurements. These results clearly indicate that there is no reaction taking place on Zn^0, different from the case utilizing Zn^IMFI. Taking these results into consideration, it is reasonable to consider that the oxidation of Zn^0 with O_2 would require a large activation energy; there is an energy barrier in the reaction between O_2 and Zn^0. This reaction will be observed at higher temperatures, as generally observed. It is recognized that triplet oxygen will readily react with molecules in a doublet state, such as radicals, to form a new radical. Therefore, the singlet state of Zn^0 may be relatively resistant to oxidation, different from the doublet state of Zn^+ in the ground state. Qualitative and detailed explanations and discussions of these concerns are difficult at the present stage.
(43) McLaren, E. H.; Helmholz, L. *J. Phys. Chem.* **1959**, *63*, 1279−1283.
(44) Känzig, W.; Cohen, M. H. *Phys. Rev. Lett.* **1959**, *3*, 509−510.
(45) Anpo, M.; Che, M.; Fubini, B.; Garrone, E.; Giamello, E.; Paganini, C. *Top. Catal.* **1999**, *8*, 189−198.
(46) Chiesa, M.; Giamello, E.; Che, M. *Chem. Rev.* **2010**, *110*, 1320−1347.
(47) Frisch, M. J.; Trucks, G. W.; Schlegel, H. B.; Scuseria, G. E.; Robb, M. A.; Cheeseman, J. R.; Montgomery, J. A., Jr.; Vreven, T.; Kudin, K. N.; Burant, J. C.; Millam, J. M.; Iyengar, S. S.; Tomasi, J.; Barone, V.; Mennucci, B.; Cossi, M.; Scalmani, G.; Rega, N.; Petersson, G. A.; Nakatsuji, H.; Hada, M.; Ehara, M.; Toyota, K.; Fukuda, R.; Hasegawa, J.; Ishida, M.; Nakajima, T.; Honda, Y.; Kitao, O.; Nakai, H.; Klene, M.; Li, X.; Knox, J. E.; Hratchian, H. P.; Cross, J. B.; Bakken, V.; Adamo, C.; Jaramillo, J.; Gomperts, R.; Stratmann, R. E.; Yazyev, O.; Austin, A. J.; Cammi, R.; Pomelli, C.; Ochterski, J. W.; Ayala, P. Y.; Morokuma, K.; Voth, G. A.; Salvador, P.; Dannenberg, J. J.; Zakrzewski, V. G.; Dapprich, S.; Daniels, A. D.; Strain, M. C.; Farkas, O.; Malick, D. K.; Rabuck, A. D.; Raghavachari, K.; Foresman, J. B.; Ortiz, J. V.; Cui, Q.; Baboul, A. G.; Clifford, S.; Cioslowski, J.; Stefanov, B. B.; Liu, G.; Liashenko, A.; Piskorz, P.; Komaromi, I.; Martin, R. L.; Fox, D. J.; Keith, T.; Al-Laham, M. A.; Peng, C. Y.; Nanayakkara, A.; Challacombe, M.; Gill, P. M. W.; Johnson, B.; Chen, W.; Wong, M. W.; Gonzalez, C.; Pople, J. A. *Gaussian 03, Revision B.03*; Gaussian, Inc., Pittsburgh, PA, 2003.
(48) Becke, A. D. *Phys. Rev.* **1988**, *A38*, 3098−3100.
(49) Becke, A. D. *J. Chem. Phys.* **1993**, *98*, 5648−5652.
(50) Stephens, P. J.; Devlin, F. J.; Chabalowski, C. F.; Frisch, M. J. *J. Phys. Chem.* **1994**, *98*, 11623−11627.
(51) Lee, C.; Yang, W.; Parr, R. G. *Phys. Rev.* **1988**, *B37*, 785−789.
(52) Levine, I. N. *Quantum Chemistry*, 5th ed.; Prentice-Hall: Upper Saddle River, NJ., 1999.
(53) The MFI structure was taken from the Cerius 2 database: *Cerius 2*; Accelerys Software, Inc., San Diego, CA.
(54) Andersson, M. P.; Uvdal, P. *J. Phys. Chem. A* **2005**, *109*, 2937−2941.